Geofísica Internacional (2001), Vol. 40, Num. 3, pp. 181-190

Crustal structure of south-central Mexico estimated from the inversion of surface-wave dispersion curves using genetic and simulated annealing algorithms

A. Iglesias, V. M. Cruz-Atienza, N. M. Shapiro, S. K. Singh and J. F. Pacheco
Instituto de Geofísica, UNAM, México, D.F., México

Received: April 23, 2001; accepted: May 16, 2001

RESUMEN

A partir de catorce sismos de subducción, agrupados en dos trayectorias (una perpendicular y otra paralela a la línea de costa), se calculó un apilado sobre las curvas de dispersión de velocidad de grupo. Estas curvas promedio fueron invertidas usando, por separado, los métodos de algoritmos genéticos y recristalización simulada. Los resultados muestran fuertes diferencias entre ambos modelos corticales, sobre todo, en los parámetros de la capa más somera y en la localización del Moho. Estas diferencias pueden ser explicadas debido a que la primera trayectoria atraviesa el terreno tectonoestratigráfico "Guerrero" y la segunda el "Oaxaca".

La inversión con algoritmos genéticos (GA) probó ser considerablemente más rápida que aquélla con recristalización simulada (SA). Por otro lado SA requiere una pequeña cantidad de memoria y alcanza un desajuste menor que G.A.

PALABRAS CLAVE: Algoritmos genéticos, recristalización simulada, dispersión, estructura cortical.

ABSTRACT

We have computed group velocities of the fundamental mode of Rayleigh waves along two paths using broadband seismograms of fourteen subduction-zone earthquakes in Mexico. One path crosses the Guerrero terrane while the other traverses the Oaxaca terrane. The dispersion curves have been inverted for crustal structure using genetic and simulated annealing algorithms. Our results show significant differences in crustal structure beneath the Guerrero and the Oaxaca terranes, especially in velocity of the superficial layer and Moho depth. The genetic algorithm (GA) is considerably faster than the simulated annealing algorithm (SA). On the other hand, the SA requires a small computer memory. Another significant advantage of SA is that it reaches a smaller misfit value than GA.

KEY WORDS: Genetic algorithm, simulated annealing, surface-wave dispersion, crustal structure of Mexico.

INTRODUCTION

Inverse problems in geophysics have often been solved using linear methods. In many geophysical problems classical least-squares inversion has proved to be a useful tool in extracting information from observed data. However, when the forward problem is non-linear the classical inversion requires expanding in Taylor series which makes it difficult for the solution to converge to the global minimum, especially if the *a priori* information is sparse. Recent advances in computational capabilities allow the use of optimization techniques which explore the entire solution domain to find the global minimum. Although these techniques often require a large computational effort, they are preferable to nonlinear inversion. Simulated Annealing (SA) (Kirkpatrick *et al.*, 1983) and Genetic Algorithm (GA) (Holland, 1975) are two semi-global optimization methods that can be easily implemented to solve many geophysical inverse problems. Recently, these methods have been used to determine earthquake source parameters (Hartzell and Liu, 1995), to obtain elastic properties from waveforms (e.g. Sambridge and Drijoningen, 1992; Zhou *et al.*,1995), and to estimate resistivity properties (Sen *et al.*, 1993). In this study, we apply these methods to invert surface wave dispersion curves for crustal structure in two regions of Mexico.

The main idea of a genetic algorithm (Holland, 1975 and Goldberg, 1989) is to translate the common genetic process (selection, crossover, and mutation) into a computational language to apply in optimization problems. Each model (set of parameters) is codified in a binary scheme, simulating the genetic information of an organism. Forward problem is computed and the theoretical response is compared with observed data using some misfit function. A selection process, based on misfit for each model, simulates the death risk of an organism from predators. Only those models whose misfit values are small remain in the inversion process. After selection, the information contained in the genetic chain is interchanged between pairs of models. This is similar to sexual reproduction in natural evolution; it permits the diversity of models. Finally, the parity of some bit is changed over some models, simulating the mutation process which occur in the

nature. All of these procedures are included in an iterative scheme, which stops when some desired misfit criterion is reached.

The simulated annealing method, developed by Kirkpatrick *et al.* (1983), attempts to reproduce the annealing process. When a mineral substance is slowly cooled, crystals are formed. If it is rapidly frozen only glasses are obtained. This principle leads to a computational algorithm to perform nonlinear inversion. By perturbing an initial model, the algorithm computes the forward problem and the misfit between data and synthetics. The misfit value of a new model may be higher than the misfit value for the initial model; however, its existence is determined by computing a probability based on an "energy" function (Vasudevan *et al.*, 1991), which depends on the misfit and also on a constant, which may be denoted temperature. This procedure is equivalent of computing the existence probability of a specific configuration in a thermodynamic process. It allows to escape from local minimums. The process is iterative as the temperature parameter is slowly reduced.

In this paper, we apply both techniques to surface-wave dispersion curves to obtain crustal structure beneath Guerrero and Oaxaca. Several studies deal with the seismic velocity structure in different locations of Mexico (e.g. Fix, 1975; Valdés *et al.*, 1986; Gomberg *et al.*, 1988; Nava *et al.*, 1988; Campillo *et al.*, 1989; Valdés and Meyer, 1996), but knowledge of the structure is still lacking in many regions. Some information can be obtained from some tomographic studies which cover Mexico (Van der Lee and Nolet, 1997; Vdovin *et al.*, 1999). However, because of large uncertainties and poor spatial resolution, these studies do not provide precise information on crustal and upper mantle structure.

Campa & Cooney (1983) distinguish between several tectonostratigraphic terranes in Guerrero and Oaxaca (Figure 1). The basement of the Oaxaca terrane, called the Oaxaca Complex, is formed by Precambrian metamorphic rocks. The basement of Mixteco and Guerrero terranes (the Acatlan Complex) consists of early Paleozoic metasediments covered by Mesozoic volcanic and sedimentary sequences.

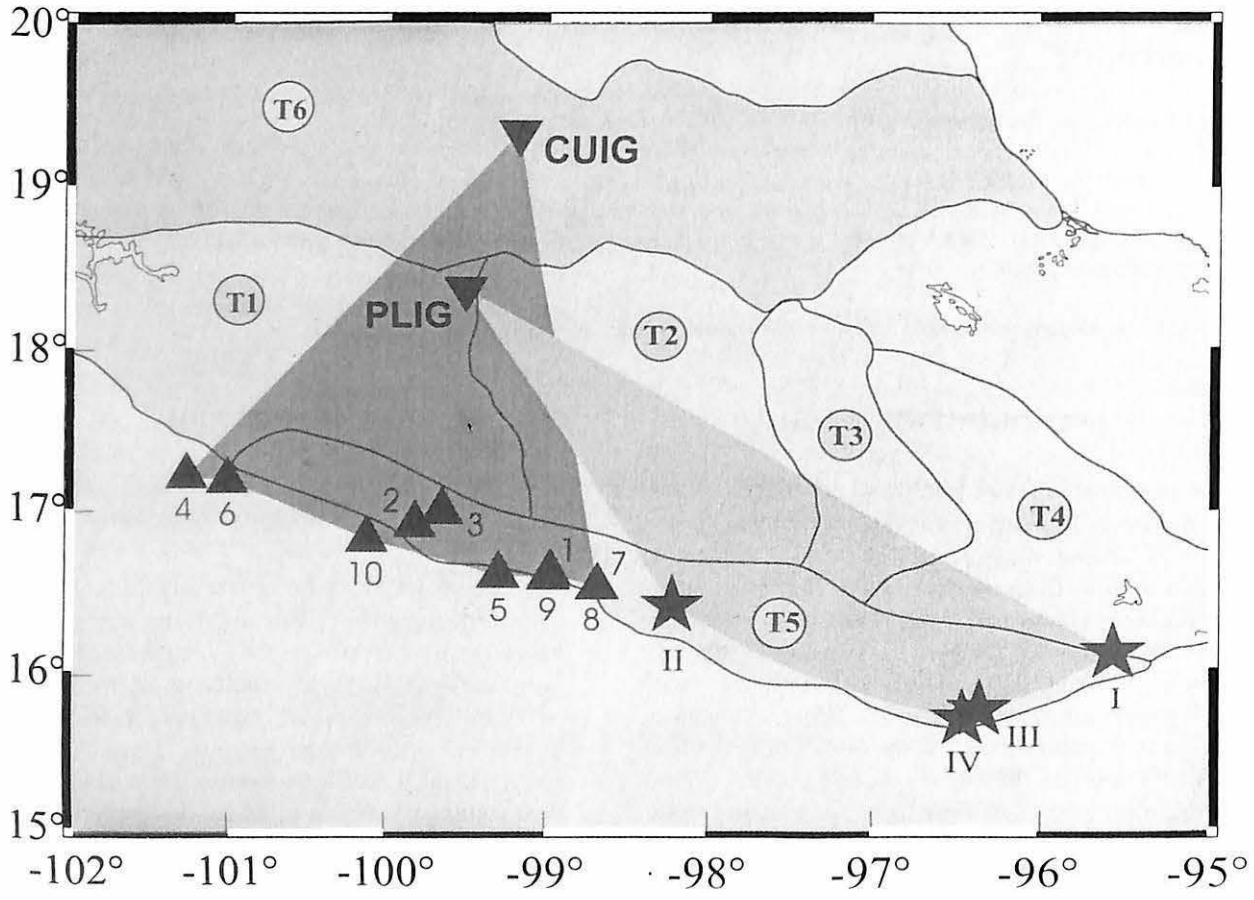

Fig. 1. Epicenters of the fourteen events listed in Table 1 and the locations of the two stations used in this study. The events, which lie in the shaded sector with apex at station CUIG, are grouped together. The wave paths in this sector belong to path 1. Similarly, the events lying in the shaded sector with apex at PLIG are grouped together and the wave paths belong to path 2. The circled numbers indicate tectonostratigraphic terranes. T1: Guerrero, T2: Mixteco, T3: Oaxaca, T4: Zapoteco, T5: Xolapa, and T6: Mexican Volcanic Belt (Campa and Cooney, 1983). Although paths 1 and 2 cross several terranes, for simplicity path 1 is assigned to Guerrero and path 2 to Oaxaca.

We have obtained records of 14 subduction-zone earthquakes along two paths, one crossing the Mixteco-Guerrero terrane and the other crossing mostly the Xolapa-Mixteco terrane (Figure 1). The terranes covered by paths 1 and 2 are referred as Guerrero and Oaxaca, respectively. We have measured the group velocity of the fundamental Rayleigh mode along each of the paths. As mentioned above, we apply the genetic and the simulated annealing methods to obtain the crustal structure from the measured surface waves dispersion curves. Some modifications have been made to the classical SA and GA schemes. A comparison of the two methods is made in terms of speed, memory requirements, and convergence efficiency.

DATA AND PROCESSING

We use vertical-component seismograms (Table 1) to measure group velocities of the fundamental mode of the Rayleigh wave. The seismograms are divided in two groups. One group consists of ten well-located events along the Guerrero coast recorded at station CUIG in Mexico City. Seismograms from this group are used to determine the structure of the Guerrero terrane. The second group of events, used to find the structure of the Oaxaca terrane, consists of four events located near the coast of Oaxaca recorded at station PLIG situated near Iguala. The locations and magnitudes of these events were taken from the catalog of the Servicio Sismológico Nacional.

The locations of stations and events are shown in Figure 1. Both stations are part of the Mexican broadband seismological network (Singh *et al.*, 1997).

We use the multiple filter technique (Dziewonski *et al.*, 1969) and logarithmic stacking (Campillo *et al.*, 1996; Shapiro *et al.*, 1997) to compute stacked dispersion curves of the fundamental mode of Rayleigh waves for both paths. The multiple filter technique consists of the application of a set of Gaussian amplitude filters with different central frequencies to the input spectrum, followed by calculation of inverse Fourier transforms. The group arrival times are estimated from the maxima of the time envelopes. It is known that this method leads to a systematic error in the group-velocity measurements (Levshin *et al.*, 1989) due to the wrong frequency assignation related with the variation of spectral amplitude, which shifts the central frequency of the filtered spectrum. To avoid this error, we apply a correction proposed by Shapiro and Singh (1999) for the frequency assignation of each group velocity value. It consists of the computation of a centroid frequency, which is the frequency where the filtered spectrum attains its maximum. The filtered spectrum is assigned to this centroid frequency.

The logarithmic stacking consists of multiplication of the normalized amplitudes of the spectrum in the group-time domain. It provides an average dispersion curve and the standard deviation at each computed period. Figure 2 shows stacked dispersion curves for both paths at periods between 5 and 45 s.

Table 1

List of Events

	Date mm/d/y	Latitude (N)	Longitude (W)	Depth (Km)	M
		Path 1			
1	4/21/91	16.61	98.98	16.0	4.2
2	5/28/91	16.92	99.82	27.2	3.6
3	1/9/92	17.00	99.65	30.2	4.7
4	3/31/92	17.22	101.27	11.0	5.1
5	12/24/92	16.62	99.29	18.4	4.8
6	3/31/93	17.19	101.01	6.0	4.8
7	5/15/93	16.55	98.68	15.6	5.6
8	5/15/93	16.55	98.68	15.6	5.6
9	24/10/93	16.63	98.97	34.6	6.5
10	7/5/98	16.83	100.12	5.0	4.9
		Path 2			
I	1/8/97	16.13	95.57	36.0	4.6
II	1/21/97	16.43	98.22	20.0	4.7
III	2/3/98	15.77	96.36	32.9	6.4
IV	3/3/98	15.71	96.46	12.3	4.9

INVERSION

Some details of the implementation of GA and SA methods to our problem are given in Appendix A, respectively. Here we describe some modifications done to the schemes originally proposed by Rodríguez-Zúñiga *et al.* (1997) and Goffe *et al.* (1994), as applied in this work.

Time Saving. Because of the discrete model space, the selection process in GA inversion can lead to the repetition of models in different generations. This results in duplicate forward problem computations for the same model. To avoid these duplications we ensure that the algorithm computes the forward problem for each model just once, even if it appears repeatedly in the current or the last generation. This saves a significant amount of time since the forward problem computation consumes a major part of the total inversion time.

Misfit Function. The classical least-square inversion is based on the L2 norm and it implies an L2-type misfit func-

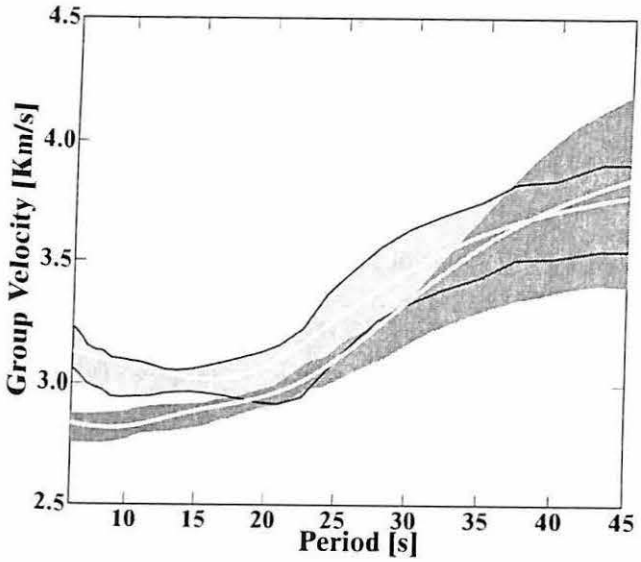

Fig. 2. Stacked dispersion curves and uncertainties for path 1 (dark) and path 2 (light shading).

tion. In semi-global inversion it is possible to select any misfit function. In our scheme, for both GA and SA, we chose the semblance between the data and the synthetics as the misfit function.

The semblance is defined by

$$cost = 0.5 - \frac{cross(obs, synth)}{auto(obs) + auto(synth)}$$

where *cost* is the semblance-misfit, *cross* is the cross-correlation, *auto* is the auto-correlation, *obs* are the observations and *synth* are the synthetics.

When the fit between data and synthetics is poor, the cross-correlation is close to zero and the semblance tends to 0.5. On the other hand, the semblance vanishes when the fit between the data and the synthetics is good.

Uncertainty Estimation in Global Search. In linear inversion it is possible to compute resolution matrices to estimate the uncertainty in model parameters (Menke, 1984). In global inversion, computation of the partial derivatives respect to the parameters is not carried out and thus the computation of resolution matrices is not feasible. To overcome this problem, we propose a method to measure the uncertainty of the inversion by taking into account the uncertainty in the data. During inversion, we keep all models whose theoretical response lies inside the error band defined by the standard deviation of the stacked dispersion curves. As a result, we do not obtain one model but a set of acceptable models. For practical purposes, it is convenient to have a representative model of the entire set. Assuming that a Gaussian distribution can represent the set of acceptable models, we compute an average model and an uncertainty of each parameter. Using this procedure, we take into account the uncertainty in the observed stacked dispersion curve to evaluate the quality of our results.

GROUP VELOCITY INVERSION

As in similar works (*e.g.*, Campillo *et al.*,1996), we restrict the models to three layers overlying a half space for both paths. We invert for the S-wave velocity of each layer and the interface depths. A Poisson ratio of 0.25 is assumed in all layers. The densities are computed from the relation given by Berteussen (1977):

$\rho = 0.32\alpha + 0.77$, where α is the P-wave velocity in $\frac{Km}{s}$ and ρ is the density in $\frac{gr}{cm^3}$.

The possible variations in each parameter were restricted based on *a priori* information from previous works (e.g., Valdés *et al.*, 1986; Campillo *et al.*, 1989; Campillo *et al.*, 1996; Valdés and Mayer, 1996).

Figures 3a and 3b show the inverted S-wave velocity models for paths 1 and 2, respectively. Dotted lines show the pre-established limits for each parameter. Gray lines show all acceptable models. Solid lines represent the average models and the shaded area gives the standard deviation. The dashed-dotted line is the model determined by Campillo *et al.* (1996) for the region between the Guerrero coast and Mexico City. Average values and standard deviations of the parameters of the model for each path, assuming a Gaussian distribution, are listed in Table 2. This procedure gives some idea of the resolution of different parameters of the model. For example, Moho depths in the inverted models for Path 1 show a large variation (Figure 3a), implying poor resolution of this parameter. This is also reflected in the relatively large standard deviation of the depth to Moho.

Note that the average model for path 1 (model 1) is different from that obtained by Campillo *et al.* (1996), although the data used in both studies are similar. The difference arises from the correction applied in the present study to the systematic error in the computation of dispersion curve discussed by Shapiro and Singh (1999) as mentioned above. The average model obtained for path 2 (model 2) can be reduced to a model with two layers over a half-space, since the contrast between the superficial and the second layer is negligible. Important differences between models 1 and 2 are (1) A superficial layer with a slightly reduced velocity for path 1, which is absent for path two. This layer can be attributed to the meta-sedimentary rocks forming the shallow part

Table 2

Parameters and uncertainties of average models.

	PATH 1				PATH 2			
Layer	*Thickness (Km)*	σ	β *(Km/s)*	σ	*Thickness (Km)*	σ	β *(Km/s)*	σ
1	8.75	1.134	3.19	0.031	5.20	0.871	3.45	0.031
2	10.35	1.662	3.46	0.050	10.50	1.936	3.50	0.044
3	23.26	2.502	3.96	0.084	18.00	1.845	3.75	0.060
Half-Space	∞	-	4.80	0.14	∞	-	4.45	0.015

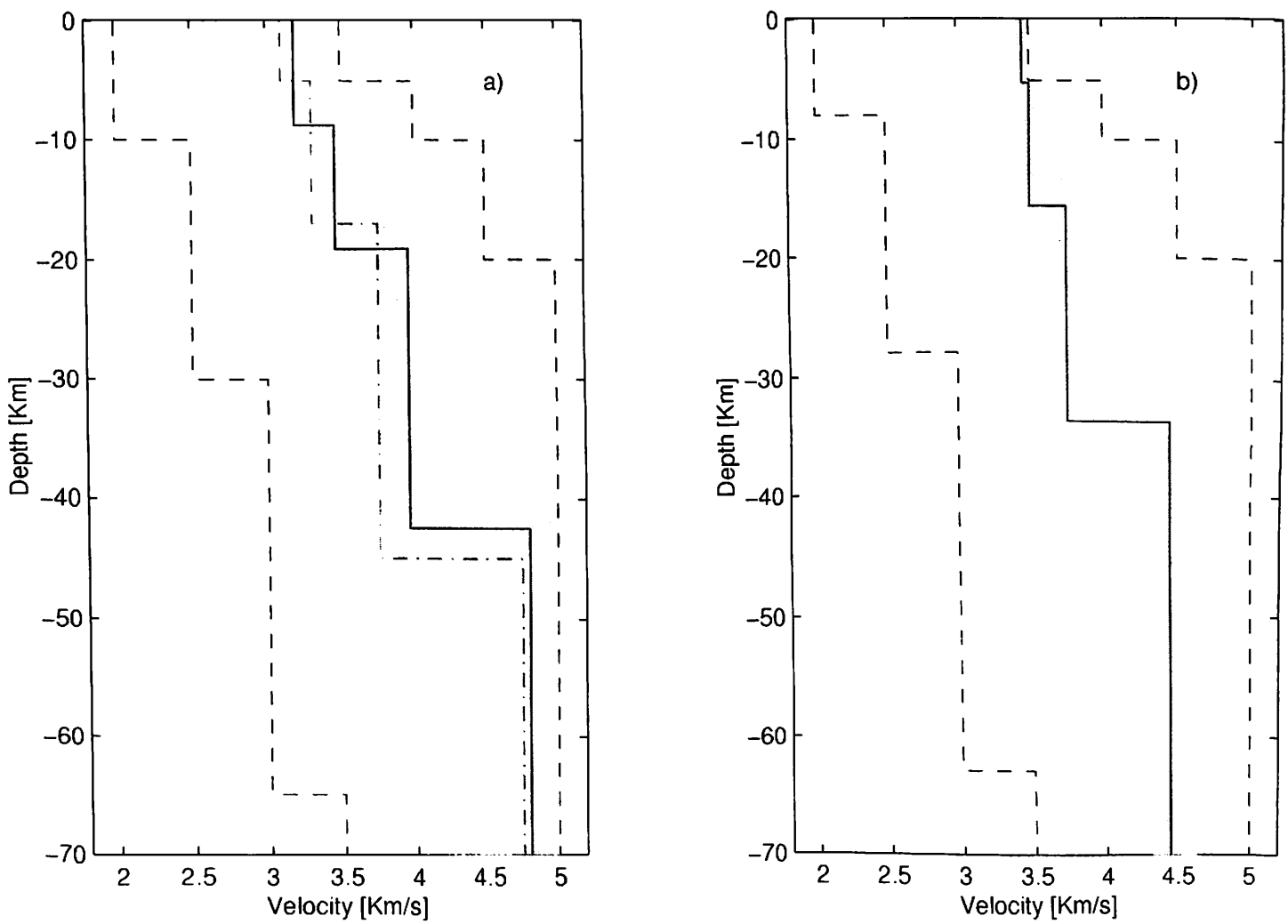

Fig. 3. Average shear-wave velocity model. (a) path 1, Guerrero and (b) path 2, Oaxaca. Dashed lines show the pre-established limits for each parameter. Gray lines indicate all acceptable models. Solid line represents the "average" model and the shaded area gives its standard deviation. The dashed-dotted line is the model reported by Campillo *et al.* (1996) for the region between the Guerrero coast and Mexico City.

of the Guerrero terrane; (2) A shallower Moho depth in model 2 than in model 1. This result is in agreement with the model found by Valdés *et al.* (1986) for Oaxaca. In this model, the continental crust is thinner near the coast. The difference in the crustal structure probably reflects the different evolution of the Guerrero and the Oaxaca terranes.

COMPARISON OF GA AND SA INVERSION TECHNIQUES

With the modifications mentioned earlier, the GA inversion is 30% faster than the SA inversion. On the other hand, GA needs more memory as compared to SA. In problems involving a large number of parameters, a small computer might be insufficient for GA. A further advantage of the SA inversion is that it converges with a lesser misfit as compared to the GA inversion, the reason being that GA uses discrete grids. Figure 4 shows a convergence comparison, relative computation times, and memory requirements.

CONCLUSIONS

We have measured group-velocity dispersion curves of Rayleigh waves for two paths in south-central Mexico. One path crosses the Guerrero terrane, while the other traverses the Oaxaca terrane (Figure 1). The measured dispersion curves have been inverted for S-wave velocity structure using genetic and simulated annealing algorithms. The results for the two different methods are very similar. For Guerrero, the average model consists of a superficial layer shear-wave velocity (~3.12 km/s) that can be attributed to Cretaceous rocks. The Moho discontinuity is located at a depth of ~43 km. The superficial layer is not observed in Oaxaca and the Moho discontinuity is shallower (~34 km). Thus our analysis shows significant differences in the crust below Guerrero and Oaxaca.

We have tested the efficiency of the GA and SA inversion methods. We find that GA saves 30% of computation time as compared to SA. On the other hand, SA requires smaller memory and shows better convergence during the final iterations.

APPENDIX

Genetic Algorithm

Our implementation of the genetic algorithm is similar to that proposed by Rodríguez-Zúñiga *et al.* (1996)

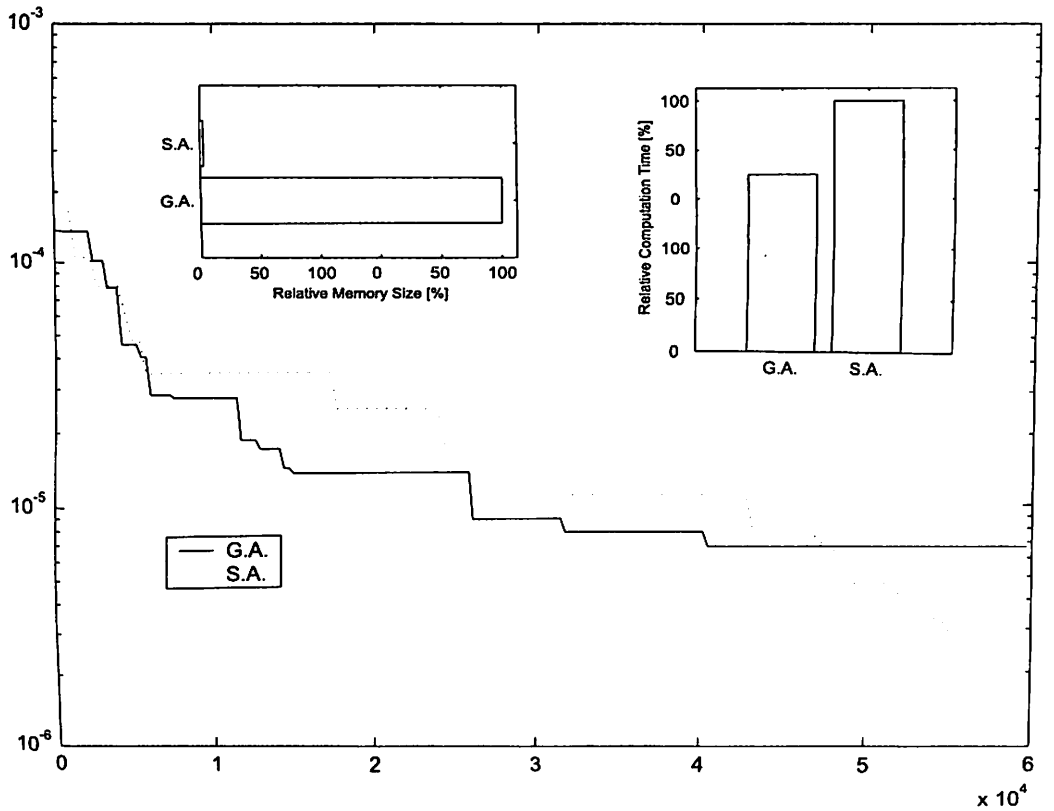

Fig. 4. Misfit evolution of genetic algorithm (solid line) and simulated annealing technique(dotted line). The insets show the relative compute time and memory size.

(a) Solution space discretization and random initial population. The solution space is defined by *a priori* information. To discretize the space, an increment for each parameter is established. The allowed values of each parameter are computed from

$$x_i = x_0 + [i * \Delta]$$

where x_i=i^{th} value of the x parameter, x_0= first value of the x parameter, and Δ = increment of the x parameter.

A model is a combination of parameters, which is codified into a binary string. A random initial population is determined. The user controls the initial population size which remains the same during the inversion.

(b) Forward modeling and misfit function.

The algorithm computes the forward problem and the misfit for every model of the initial population. In our case, the forward problem was solved using the set of surface wave programs in Herrmann (1987). We chose the semblance (see above) as the misfit function.

(c) Selection.

Our selection procedure consists of computing a survival probability for each model following the "biased roulette" criterion (Goldberg, 1989).

(d) Crossover.

Genetic strings of a pair of models are cut at a point selected randomly and then interchanged. This procedure is followed for all models.

(e) Mutation

Mutation is the change of parity over one bit for some models. The number of mutations depends of the stage of the process and follows the relation (Yamanaka and Ishida, 1996):

$$\gamma = \frac{1}{M}\sum_{i=1}^{M}\left(\frac{\sigma_i}{\bar{x}}\right)$$

where γ is the mutation probability, M is the number of parameters, $\bar{x}$ is the average over parameter i and σ_i is the standard deviation over parameter i.

To avoid unnecessary computation, the forward problem for models evaluated in a generation is not recomputed. This procedure permits saving of at least 30% in computation time. Figure A (left) shows a flow diagram of our genetics algorithm.

Simulated Annealing Method

Our implementation is similar to that proposed by Goffe *et al.* (1994)

(a) For an initial model we compute the solution of the forward problem and its misfit function (as in GA).

(b) The model parameters are perturbed so that

$$x_i = x_{i-1} * VM(i)rand,$$

where x_i is the vector of model parameters for the i-th iteration, VM is a vector which contains the maximum-step perturbation and *rand* is a random number between 0 and 1. The user initializes this vector and the program adjusts the values depending on temperature.

(c) For the new perturbed model, the forward problem is solved and the misfit function is computed. The new model will replace the initial model according to the Metropolis criteria:

$$P_s\begin{cases} e^{\frac{-\Delta E}{T}} & \Delta E > 1 \\ 1 & \Delta E < 1, \end{cases}$$

where P_s is the probability of a model to replace the initial model, ΔE is the difference in the misfit of the initial model and the perturbed model, and T is the initial temperature of the process.

The control goes to the initial point and steps (a) to (c) are repeated intercalating VM adjustment and reduction of temperature according to

$$T_{new} = T_{previous} * RT,$$

where RT is a number close to but less than one.

The algorithm stops when the misfit is less than some pre-established value, or when the maximum number of iterations is reached. Figure A (right) shows a flow diagram of our implementation of simulated annealing.

AKNOWLEDGEMENTS

We thank to C. Lomnitz for his revision and his useful comments on the manuscript. We are grateful to SSN to pro-

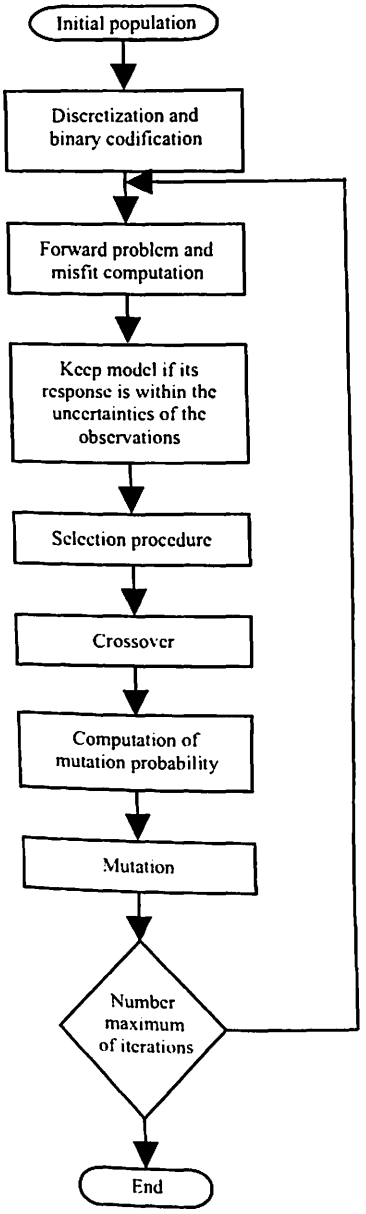

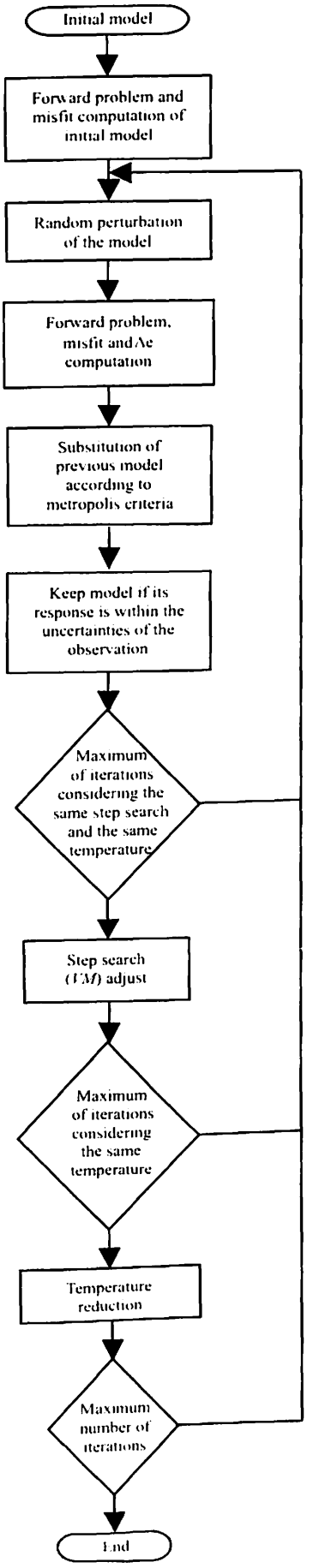

Fig. A. Flow diagram of our implementation of genetic algorithm (left) and simulated annealing (right).

vide the data for this work. This work was partially supported by DGAPA, UNAM project IN105199 and CONACyT project 26185T.

BIBLIOGRAPHY

BERTEUSSEN, K. A., 1977. Moho depth determination based on spectral ratio analysis of NORSAR long-period P waves. *Phys. Earth Planet Inter., 31*, 313-326

CAMPA, M. F. and P. J. CONEY, 1983. Tectonic-stratigrafic terranes and mineral resource distributions in Mexico. *Can. J. Earth Sci. 20*, 1040-1051

CAMPILLO, M., J. C. GARIEL, K. AKI and F. J. SANCHEZ-SESMA, 1989. Destructive strong ground motion in Mexico City: Source, site and path effects during the great 1985 Michoacán earthquake. *Bull. Seism. Soc. Am. 79*, 1718-1735.

CAMPILLO, M., S. K. SINGH, N. SHAPIRO, J. PACHECO and R. B. HERMANN, 1996. Crustal structure of the Mexican volcanic belt, based on group velocity dispersion. *Geofís. Int., 35*, 4, 361-370.

DZIEWONSKI, A., S. BLOCH and M. LANDISMAN, 1969. A technique for the analysis of transient seismic signals. *Bull. Seism. Soc. Am., 59*, 427-444.

FIX, J. E., 1975. The crust and upper mantle of central Mexico. *Geophys. J.R. Astr. Soc., 43*, 453-500.

GOFFE, W., G. D. FERRIER and J. ROGERS, 1994. Global optimization of statistical functions with simulated annealing. *Journal of Econometrics, 60*, 65-100.

GOLDBERG, D. E., 1989. Genetic algorithms in search. Optimization and machine learning. Addison Wesley. Reading, Massachusetts.

GOMBERG, J. S., K. F. PRIESTLEY, G. MASTERS and J. N. BRUNE, 1988. The structure of the crust and upper mantle of northern Mexico. *Geophys. J., 94*, 1-20.

HARTZELL, S. and P. LIU, 1995. Determination of earthquake source parameters using a hybrid global search algorithm. *Bull. Seism. Soc. Am., 85*, 516-524.

HERRMANN, R. B., 1987. Computer programs in seismology, Volume IV: Surface waves, Saint Louis University, Missouri.

HOLLAND, J., 1975. Genetic algorithms, *Scientific American*, July, 44-50

KIRKPATRICK, S., C. D. GELLAT JR. and M. P. VECCHI, 1983. Optimization by simulated annealing. *Science, 220*, 671-680.

MENKE, W., 1984. Geophysical data analysis: discrete inverse theory. Academic Press, Inc. Orlando.

NAVA, F. A. *et al.*, 1988. Structure of the Middle America trench in Oaxaca, Mexico. *Tectonophysics 154*, 241-255.

RODRÍGUEZ-ZÚÑIGA J. L., C. ORTÍZ-ALEMÁN, G. PADILLA and R. GAULÓN, 1997. Application of genetic algorithms to constrain shallow elastic parameters using in situ measurements. *Soil. Dyn. and Earth. Eng., 16*, 3, 223-234.

SAMBRIDGE, M. and G. DRIJONINGEN, 1992. Genetic algorithms in seismic waveform inversion. *Geophys. J. Int., 109*, 323-342.

SINGH S. K., J. PACHECO, F. CORBOULEX and D. A. NOVELO, 1997. Source Parameters of the Pinotepa Nacional, Mexico, earthquake of 27 March, 1996 (Mw=5.4) estimated from near-field recordings of a single station. *Journal of Seismology, 1*, 39-45.

SEN, M. K., B. BIMALENDU and P. L. STOFFA, 1993. Nonlinear inversion of resistivity sounding data. *Geophysics, 58*, 1-12.

SHAPIRO, N., M. CAMPILLO, A. PAUL, S. K. SINGH, D. JONGMANS and F. J. SÁNCHEZ-SESMA, 1997. Surface-wave propagation across the Mexican Volcanic Belt and the origin of the long-period seismic-wave amplification in the Valley of Mexico. *Geophys. J. Int., 128*, 151-166.

SHAPIRO, N. M. and S. K. SINGH, 1999. A systematic error in estimating surface-wave group-velocity dispersion curves and a procedure for its correction. *Bull. Seism. Soc. Am., 89*, 1138-1142.

VALDÉS, C. M., W. D. MOONEY, S. K. SINGH, R. P. MAYER, C. LOMNITZ, J. H. LUETGERT, B. T. HELSLEY, B. T. R. LEWIS and M. MENA, 1986. Crustal structure of Oaxaca, Mexico from seismic refraction measurements. *Bull. Seism. Soc. Am., 76*, 547-564.

VALDÉS, C. M. and R. P. MEYER, 1996. Seismic structure between the Pacific coast and Mexico City from the Petatlán earthquake (Ms=7.6) aftershocks. *Geofís. Int.*, *35*, 4, 377-401.

VAN der LEE, S. and G. NOLET, 1997. Upper mantle S velocity structure of North America, 1997. *J. Geophys. Res.-Sol.*, *102*, 22815-22838.

VDOVIN, O, J. A. RIAL, A. L. LEVSHIN and M. H. RITZWOLLER, 1999. Group-velocity tomography of South America and the surrounding oceans. *Geophys. J. Int.*, *136*, 324-340.

ZHOU, R., F. TAJIMA and P. STOFFA, 1995. Application of genetic algorithms to constrain near-source velocity structure for the 1989 Sichuan earthquakes. *Bull. Seism. Soc. Am.*, *85*, 590-605.

A. Iglesias, V. M. Cruz-Atienza, N. M. Shapiro, S. K. Singh and J. F. Pacheco
Instituto de Geofísica, UNAM, México D.F., México.
Email: amg@ollin.igeofcu.unam.mx